Analysis of Starlink Satellite Altitudes Using Quantum Gravity Theory with Ultimate Acceleration

Huaiyang Cui
Department of Physics, Beihang University, Beijing, 102206, China
Email: hycui@buaa.edu.cn
(July 31 2022 version 1; October 1 2023 version 2, submitted to viXra)

Abstract: In analogy with the ultimate speed *c*, there is an ultimate acceleration β, nobody's acceleration can exceed this limit β, in the solar system, β=2.956391e+10(m/s^2). Because this ultimate acceleration is a large number, any effect connecting to β will become easy to test, including quantum gravity tests. In this paper, an approach is put forward to connect the ultimate acceleration with quantum theory, as an application, the quantum gravity theory with the ultimate acceleration provides a useful formula to calculate the space debris distribution around the earth, in this paper the calculation results agree well with the experimental observation. Between February 2018 and 2022, SpaceX successfully launched 2,091 satellites into orbit. In March 2020, SpaceX reported producing six satellites per day. Comparing to the space debris distribution, Starlink satellite altitudes are analyzed, some suggestions can be made to improve the Starlink constellation design and status by the quantum gravity theory with the ultimate acceleration.

1. Introduction

Some quantum gravity proposals [1,2] are extremely hard to test in practice, as quantum gravitational effects are appreciable only at the Planck scale [3]. But ultimate acceleration gives another scheme to deal with quantum gravity effects.

In analogy with the ultimate speed *c*, there is an ultimate acceleration β, nobody's acceleration can exceed this limit β, in the solar system, β=2.956391e+10(m/s^2). Because this ultimate acceleration is a large number, any effect connecting to β will become easy to test, including quantum gravity tests.

In recent years, de Broglie matter wave has been generalized in terms of the ultimate acceleration, and applied to the solar system to explain quantum gravity effects [28,29]. Consider a particle, its relativistic matter wave is given by the path integral

$$\psi = \exp(\frac{i\beta}{c^3}\int_0^x (u_1 dx_1 + u_2 dx_2 + u_3 dx_3 + u_4 dx_4)) \quad . \tag{1}$$

where u is the 4-velocity of the particle, β is the ultimate acceleration determined by experiments. The β replaces the *Planck constant* in this quantum gravity theory so that *its wavelength becomes a length on planetary-scale*. The early paper [30] shows that this generalized matter wave can explain the solar quantum gravity effects correctly, such as sunspot cycle, atmospheric circulation and human lifespan. The present paper shows that this quantum gravity theory with the ultimate acceleration provides a useful formula to calculate

the space debris distribution around the earth, in this paper the calculation results agree well with the experimental observation.

Between February 2018 and 2022, SpaceX successfully launched 2,091 satellites into orbit. In March 2020, SpaceX reported producing six satellites per day. The deployment of the first 1,440 satellites was planned in 72 orbital planes of 20 satellites each, with a requested lower minimum elevation angle of beams to improve reception [34]. Comparing to the space debris distribution, Starlink satellite altitudes are analyzed, some suggestions can be made to improve the Starlink constellation design and status by the quantum gravity theory with the ultimate acceleration.

2. Extracting ultimate acceleration from the solar system

In the orbital model as shown in Fig.1(a), the orbital circumference is n multiple of the wavelength of the planetary-scale relativistic matter wave, according to Eq. (1), consider a planet, we have

$$\left.\begin{aligned} \frac{\beta}{c^3}\oint_L v_l dl = 2\pi n \\ v_l = \sqrt{\frac{GM}{r}} \end{aligned}\right\} \Rightarrow \quad \sqrt{r} = \frac{c^3}{\beta\sqrt{GM}}n; \quad n = 0,1,2,\ldots \ . \tag{2}$$

This orbital quantization rule only achieves a half success in the solar system, as shown in Fig.1(b), the Sun, Mercury, Venus, Earth and Mars satisfy the quantization equation; while other outer planets fail. But, since we only study quantum gravity effects among the Sun, Mercury, Venus, Earth and Mars, so this orbital quantization rule is good enough as a foundational quantum theory. In Fig.1(b), the blue straight line expresses a linear regression relation among the quantized orbits, so it gives β=2.956391e+10 (m/s^2) by fitting the line. The quantum numbers n=3,4,5,... were assigned to the solar planets, the sun was assigned a quantum number n=0 because the sun is in the **central state**.

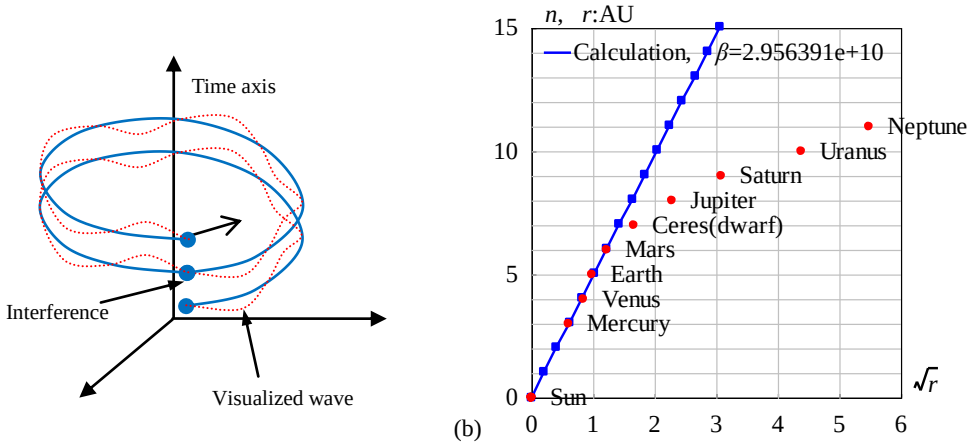

Fig.1 (a)The head of the relativistic matter wave may overlap with its tail. (b) The inner planets are quantized.

In the solar interior, if the coherent length of the relativistic matter wave is long enough, its head may overlap with its tail when the particle moves in a closed orbit, as shown in Fig.1(a).

Consider a point on the solar equatorial plane, the overlapped wave is given by

$$\psi = \psi(r)T(t)$$

$$\psi(r) = 1 + e^{i\delta} + e^{i2\delta} + ... + e^{i(N-1)\delta} = \frac{1-\exp(iN\delta)}{1-\exp(i\delta)} \quad . \tag{3}$$

$$\delta(r) = \frac{\beta}{c^3}\oint_L (v_l)dl = \frac{2\pi\beta\omega r^2}{c^3}$$

where N is the overlapping number which is determined by the coherent length of the relativistic matter wave, δ is the phase difference after one orbital motion, ω is the angular speed of the solar self-rotation. The above equation is a multi-slit interference formula in optics, for a larger N it is called as the Fabry-Perot interference formula.

The relativistic matter wave function ψ needs a further explanation. In quantum mechanics, $|\psi|^2$ equals to the probability of finding an electron due to Max Born's explanation; in astrophysics, $|\psi|^2$ equals to the probability of finding a nucleon (proton or neutron) *averagely on an astronomic scale*, we have

$$|\psi|^2 \propto \text{nucleon-density} \propto \rho \quad . \tag{4}$$

It follows from the multi-slit interference formula that the overlapping number N is estimated by

$$N^2 = \frac{|\psi(0)_{multi-wavelet}|^2}{|\psi(0)_{one-wavelet}|^2} = \frac{\rho_{core}}{\rho_{surface\_gas}} \quad . \tag{5}$$

The solar core has a mean density of 1408 (kg/m^3), the surface of the sun is comprised of convective zone with a mean density of 2e-3 (kg/m^3) [7]. In this paper, the sun's radius is chosen at a location where density is 4e-3 (kg/m^3), thus the solar overlapping number N is calculated to be N=593. Since the mass density $\rho(r)$ has spherical symmetry, then the $\psi(r)$ has the spherical symmetry.

Sun's angular speed at its equator is known as ω=2π/(25.05x24x3600) (s^{-1}). Its mass 1.9891e+30 (kg), well-known radius 6.95e+8 (m), mean density 1408 (kg/m^3), the constant β=2.956391e+10 (m/s^2). According to the N=593, the matter distribution of the $|\psi|^2$ is calculated in Fig.2(a), it agrees well with the general description of star's interior. The radius of the sun is determined as r=7e+8 (m) with a relative error of 0.72% in Fig.2, which indicates that the sun radius strongly depends on the sun's self-rotation.

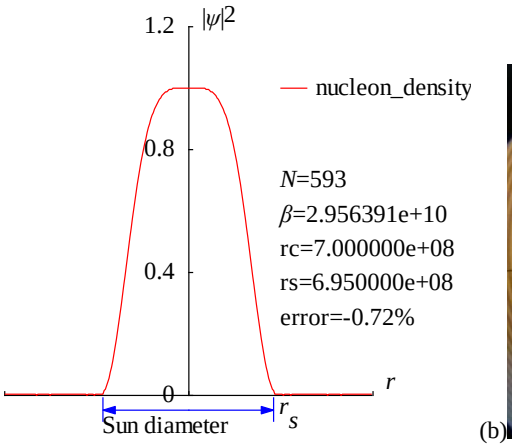

(a)

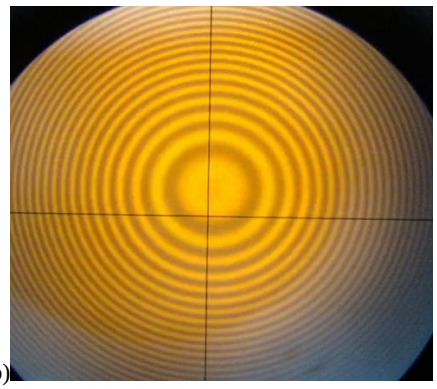

(b)

Fig.2 (a)The nucleon distribution $|\psi|^2$ in the Sun is calculated in the radius direction. (b) As contrast, sodium Fabry-Perot interference (δ=const.).

```
<Clet2020 Script>//C source code [26]
int i,j,k,m,n,N,nP[10];
double beta,H,B,M,r,r_unit,x,y,z,delta,D[1000],S[1000], a,b,rs,rc,omega,atm_height; char str[100];
main(){k=150;rs=6.95e8;rc=0;x=25.05;omega=2*PI/(x*24*3600);n=0; a=1408/0.004; N=sqrt(a);
beta=2.956391e10;H=SPEEDC*SPEEDC*SPEEDC/beta;M=1.9891E30; atm_height=2e6; r_unit=1E7;
for(i=-k;i<k;i+=1) {r=abs(i)*r_unit;
if(r<rs+atm_height) delta=2*PI*omega*r*r/H; else delta=2*PI*sqrt(GRAVITYC*M*r)/H;//around the star
x=1;y=0; for(j=1;j<N;j+=1) { z=delta*j; x+=cos(z);y+=sin(z);} z=x*x+y*y; z=z/(N*N);
S[n]=i;S[n+1]=z; if(i>0 && rc==0 && z<0.0001) rc=r; n+=2;}
SetAxis(X_AXIS,-k,0,k,"#ifr; ; ; ;");SetAxis(Y_AXIS,0,0,1.2,"#if|ψ|#su2#t;0;0.4;0.8;1.2;");
DrawFrame(FRAME_SCALE,1,0xafffaf); z=100*(rs-rc)/rs;
SetPen(1,0xff0000);Polyline(k+k,S,k/2,1," nucleon_density"); SetPen(1,0x0000ff);
r=rs/r_unit;y=-0.05;D[0]=-r;D[1]=y;D[2]=r;D[3]=y; Draw("ARROW,3,2,XY,10,100,10,10,",D);
Format(str,"#ifN#t=%d#n#ifβ#t=%e#nrc=%e#nrs=%e#nerror=%.2f%",N,beta,rc,rs,z);
TextHang(k/2,0.7,0,str);TextHang(r+5,y/2,0,"#ifr#sds#t");TextHang(-r,y+y,0,"Sun diameter");
}#v07=?>A
```

3. Extracting ultimate acceleration from the earth

Appling the planetary-scale relativistic matter wave to the Moon, as illustrated in Fig.3, The moon is assigned a quantum number of n=2 because some quasi-satellite's perigees have reached a depth almost at n=1 orbit, as shown in Fig.3. Here, the ultimate acceleration β=1.377075e+14(m/s^2) is determined uniquely by the line between the earth and moon in Fig.3 by Eq. (2).

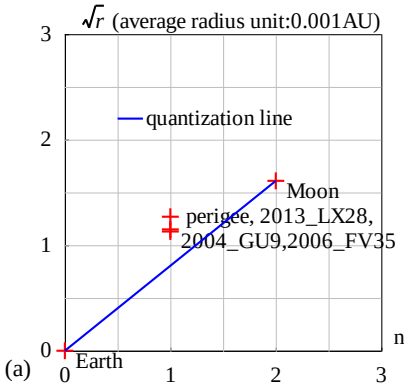

Fig.3 Orbital quantization for the moon.

```
<Clet2020 Script>// C source code [26]
char str[200];int i,j,k,N,nP[10]; double x,y,z,M,r_unit,a,b,B,H,r_ave[20],dP[10],D[1000];
double orbit[10]={0,2.57,0,}; double e[10]={0, 0.0549,0,0,0,0,0,0,0,0,};
int qn[10]={0,2,3,4,5,6,7,8,9.,10,};
char Stars[100]={"Earth;Moon;"};
int main(){ N=2; M=5.97237E24; r_unit=1.495978707e8;
for(i=0;i<N;i+=1) {x=orbit[i];y=e[i]; z=x*(1+sqrt(1-y*y))/2;r_ave[i]=z;//average_radius
D[i+i]=qn[i];D[i+i+1]=sqrt(z); }
DataJob("REGRESSION,2",D,dP);b=dP[0];a=dP[1];
SetAxis(X_AXIS,0,0,3,"n;0;1;2;3;");
SetAxis(Y_AXIS,0,0,3," #if#rsr#t (average radius unit:0.001AU);0;1;2;3;");
DrawFrame(0x0166,1,0xafffaf); Polyline(N,D);
SetPen(2,0xff0000); Plot("OVALFILL,0,2,XY,3,3,",D);
for(i=0;i<N;i+=1) {nP[0]=TAKE;nP[1]=i;TextJob(nP,Stars,str);x=qn[i]+0.2;
y=sqrt(orbit[i])-0.05;TextHang(x,y,0,str);}
x=GRAVITYC*M*r_unit;z=sqrt(x);H=z*a;B=-z*b;
TextAt(100,450,"#ifH#t=%e  #ifB#t=%e",H,B);
for(i=0;i<N;i+=1) {y=b+a*qn[i];D[i+i]=qn[i];D[i+i+1]=y;}
SetPen(1,0x0000ff);Polyline(N,D,0.5,2.2,"quantization");//check
}}#v07=?>A#t
```

Now let us talk about the earth's interior, the earth has a mean density of 5530 (kg/m^3), its surface is covered with air and vapor with a density of 1.29 (kg/m^3). The earth's radius is chosen at the sea level, it follows Eq.(5) that the earth's overlapping number N is calculated to

be N=65.

The earth's angular speed is known as $\omega=2\pi/(24\text{x}3600)$ (s^{-1}), its mass 5.97237e+24 (kg), the well-known radius is 6.378e+6 (m), the earth's constant β=1.377075e+14 (m/s^2). The matter distribution $|\psi|^2$ in radius direction is calculated by Eq.(3), as shown in Fig.4(a). The radius of the earth is determined as r=6.4328e+6 (m) with a relative error of 0.86%, it agrees well with common knowledge. Space debris over the atmosphere has a complicated evolution [7,8], has itself speed

$$v_l=\sqrt{\frac{GM}{r}};\quad \delta(r)=\frac{\beta}{c^3}\oint_L(v_l)dl=\frac{2\pi\beta}{c^3}\sqrt{GMr}\ . \tag{6}$$

The secondary peaks over the atmosphere up to 2000km altitude are calculated out in Fig.4(b) which agrees well with the space debris observations [16]; the peak near 890 km altitude is due principally to the January 2007 intentional destruction of the Fengyun-1C weather spacecraft, while the peak centered at approximately 770 km altitude was created by the February 2009 accidental collision of Iridium 33 (active) and Cosmos 2251 (derelict) communication spacecraft [16,18]. The observations based on the incoherent scattering radar EISCAT ESR located at 78 ℕ in Jul. 2006 and in Oct. 2015 [21,22,23] are respectively shown in Fig.4(c) and (d). This prediction to secondary peaks also agrees well with other space debris observations [24,25].

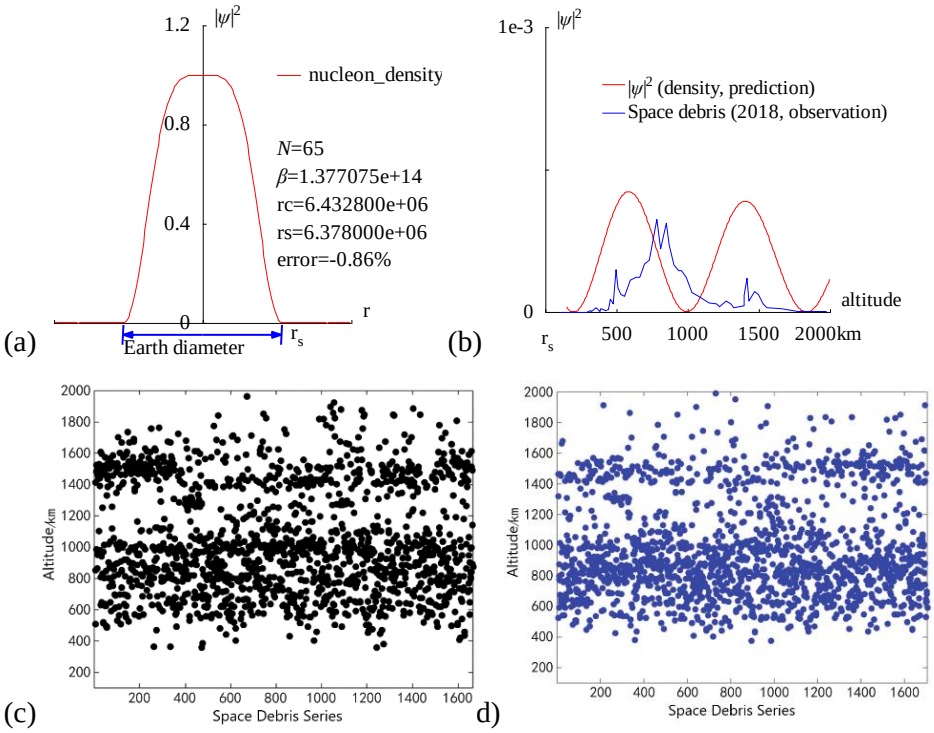

Fig.4 (a) The radius of the Earth is calculated out r=6.4328e+6 (m) with a relative error 0.86% by the interference of its acceleration-roll wave; (b) The prediction of the space debris distribution up to 2000km altitude; (c) The pace debris distribution in Jul. 2006, Joint observation based on the incoherent scattering radar EISCAT ESR located at 78 ℕ [21]; (d) The space debris distribution in Oct. 2015, Joint observation based on the incoherent scattering radar EISCAT ESR located at 78 ℕ [21].

<Clet2020 Script>//C source code [26]
int i,j,k,m,n,N,nP[10]; double H,B,M,v_r,r,AU,r_unit,x,y,z,delta,D[10],S[1000];
double rs,rc,rot,a,b,atm_height,beta; char str[100];

```
main(){k=80;rs=6.378e6;rc=0;atm_height=1.5e5;n=0; N=65;
beta=1.377075e+14;H=SPEEDC*SPEEDC*SPEEDC/beta;
M=5.97237e24;AU=1.496E11;r_unit=1e-6*AU; rot=2*PI/(24*60*60);//angular speed of the Earth
for(i=-k;i<k;i+=1) {r=abs(i)*r_unit;
if(r<rs+atm_height) v_r=rot*r*r; else v_r=sqrt(GRAVITYC*M*r);//around the Earth
delta=2*PI* v_r/H; y=SumJob("SLIT_ADD,@N,@delta",D); y=y/(N*N);
if(y>1) y=1; S[n]=i;S[n+1]=y; if(i>0 && rc==0 && y<0.001) rc=r;   n+=2;}
SetAxis(X_AXIS,-k,0,k,"r; ; ; ,");SetAxis(Y_AXIS,0,0,1.2,"#if|ψ|#su2#t;0;0.4;0.8;1.2;");
DrawFrame(FRAME_SCALE,1,0xafffaf); x=50;z=100*(rs-rc)/rs;
SetPen(1,0xff0000);Polyline(k+k,S,k/2,1," nucleon_density");
r=rs/r_unit;y=-0.05;D[0]=-r;D[1]=y;D[2]=r;D[3]=y;
SetPen(2,0x0000ff); Draw("ARROW,3,2,XY,10,100,10,10,",D);
Format(str,"#ifN#t=%d#n#ifβ#t=%e#nrc=%e#nrs=%e#nerror=%.2f%",N,beta,rc,rs,z);
TextHang(k/2,0.7,0,str);TextHang(r+5,y/2,0,"r#sds#t");TextHang(-r,y+y,0,"Earth diameter");
}#v07=?>A#t
<Clet2020 Script>//C source code [9]
int i,j,k,m,n,N,nP[10]; double H,B,M,v_r,r,AU,r_unit,x,y,z,delta,D[10],S[10000];
double rs,rc,rot,a,b,atm_height,p,T,R1,R2,R3; char str[100]; int
Debris[96]={110,0,237,0,287,0,317,2,320,1,357,5,380,1,387,4,420,2,440,3,454,14,474,9,497,45,507,26,527,19,557,17,597,34,63
4,37,664,37,697,51,727,55,781,98,808,67,851,94,871,71,901,50,938,44,958,44,991,37,1028,21,1078,17,1148,10,1202,9,1225,6,
1268,12,1302,9,1325,5,1395,7,1395,18,1415,36,1429,12,1469,22,1499,19,1529,9,1559,5,1656,4,1779,1,1976,1,};
main(){k=80;rs=6.378e6;rc=0;atm_height=1.5e5;n=0; N=65;
H=1.956611e11;M=5.97237e24;AU=1.496E11;r_unit=1e4;
rot=2*PI/(24*60*60);//angular speed of the Earth
b=PI/(2*PI*rot*rs*rs/H); R1=rs/r_unit;R2=(rs+atm_height)/r_unit;R3=(rs+2e6)/r_unit;
for(i=R2;i<R3;i+=1) {r=abs(i)*r_unit; delta=2*PI*sqrt(GRAVITYC*M*r)/H;
y=SumJob("SLIT_ADD,@N,@delta",D); y=1e3*y/(N*N);// visualization scale:1000
if(y>1) y=1; S[n]=i;S[n+1]=y;n+=2;}
SetAxis(X_AXIS,R1,R1,R3,"altitude; r#sds#t;500;1000;1500;2000km ;");
SetAxis(Y_AXIS,0,0,1,"#if|ψ|#su2#t;0; ;1e-3;");DrawFrame(FRAME_SCALE,1,0xafffaf); x=R1+(R3-R1)/5;
SetPen(1,0xff0000);Polyline(n/2,S,x,0.8,"#if|ψ|#su2#t (density, prediction)");
for(i=0;i<48;i+=1) {S[i+i]=R1+(R3-R1)*Debris[i+i]/2000; S[i+i+1]=Debris[i+i+1]/300;}
SetPen(1,0x0000ff);Polyline(48,S,x,0.7,"Space debris (2018, observation) "); }#v07=?>A#t
```

4. Planck-Constant-like Constant

The solar system, Jupiter's satellites, Saturn's satellites, Uranus' satellites, and Neptune's satellites as five different many-body systems are investigated with the Bohr's orbit model. After fitting observational data as shown in Fig.5, their ultimate accelerations are obtained and listed in Table 1. The predicted quantization blue-lines in Fig.5(a), Fig.5(b), Fig.5(c), Fig.5(d) and Fig.5(e) agree well with experimental observations for those *inner constituent planets or satellites*.

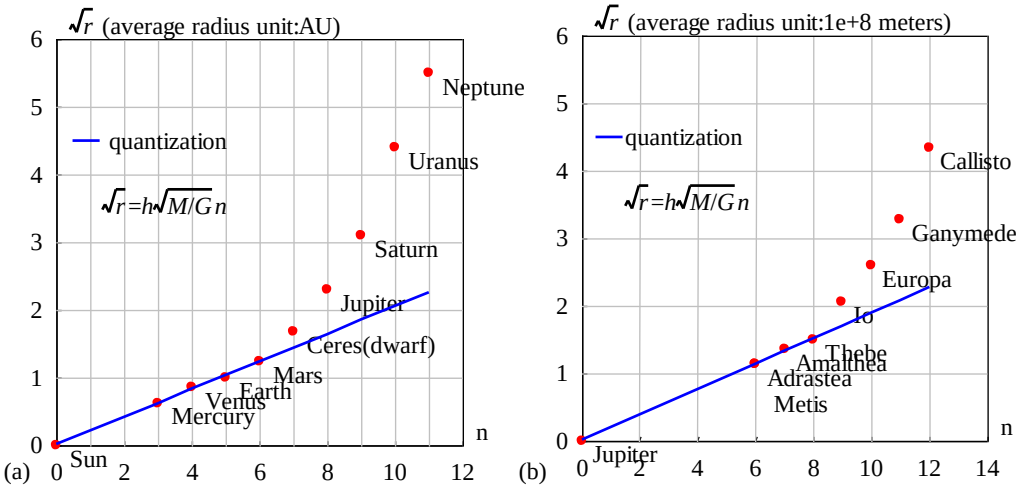

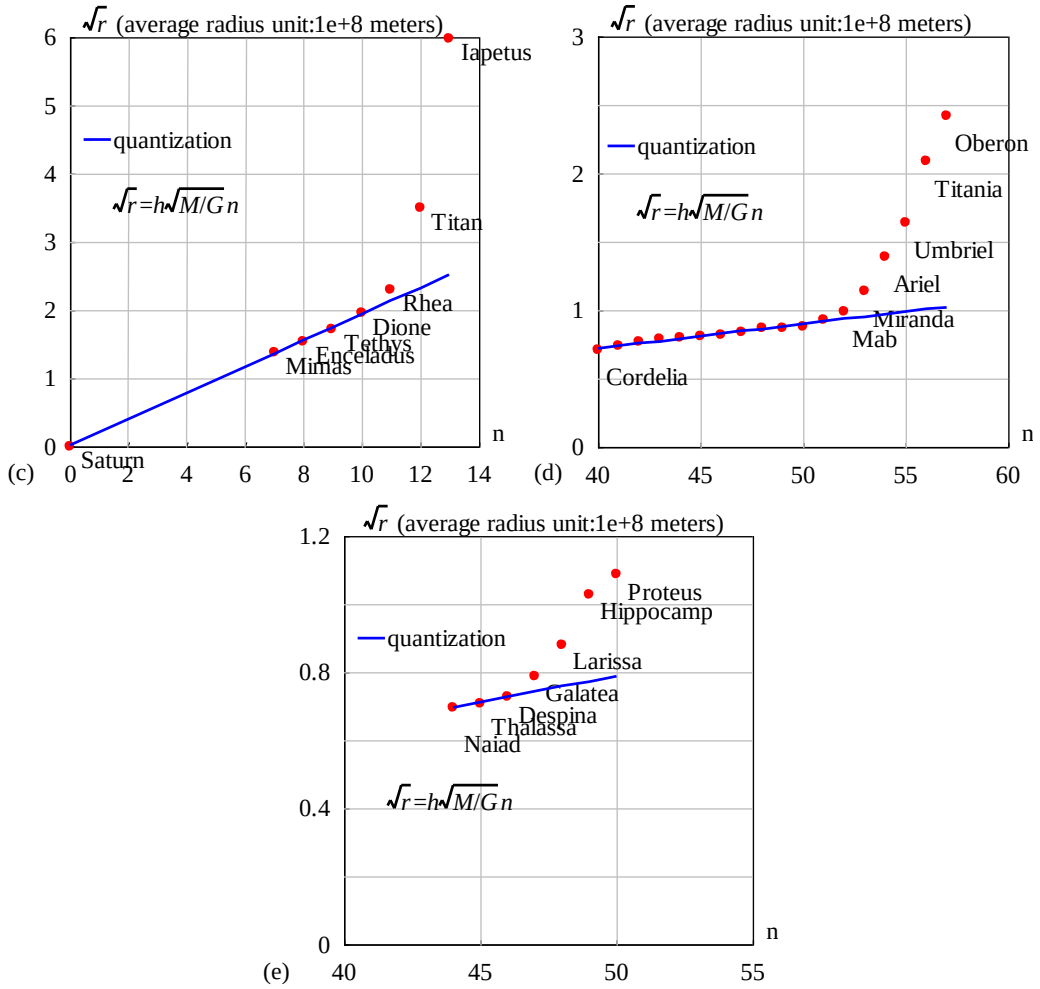

Fig.5 The orbital radii are quantized for inner constituents. (a) the solar system with h=4.574635e-16 ($m^2s^{-1}kg^{-1}$), the relative error is less than 3.9%. (b) the Jupiter system with h=3.531903e-16 ($m^2s^{-1}kg^{-1}$). Metis and Adrastea are assigned the same quantum number for their almost same radius, the relative error is less than 1.9%. (c) the Saturn system with h=6.610920e-16 ($m^2s^{-1}kg^{-1}$), the relative error is less than 1.1%. (d) the Uranus system with h=1.567124e-16 ($m^2s^{-1}kg^{-1}$). n=0 is assigned to Uranus, the relative error is less than 2.5%. (e) the Neptune system with h=1.277170e-16 ($m^2s^{-1}kg^{-1}$). n=0 is assigned to Neptune, the relative error is less than 0.17%.

Table 1 Planck-constant-like constant h, N is constituent particle number with smaller inclination.

system	N	M/M_{earth}	β (m/s^2)	h ($m^2s^{-1}kg^{-1}$)	Prediction
Solar planets	9	333000	2.961520e+10	4.574635e-16	Fig.5(a)
Jupiter' satellites	7	318	4.016793e+13	3.531903e-16	Fig.5(b)
Saturn's satellites	7	95	7.183397e+13	6.610920e-16	Fig.5(c)
Uranus' satellites	18	14.5	1.985382e+15	1.567124e-16	Fig.5(d)
Neptune 's satellites	7	17	2.077868e+15	1.277170e-16	Fig.5(e)

Besides every β, our interest shifts to the constant h in Table 1, which is defined as

$$h = \frac{c^3}{M\beta} \quad . \tag{7}$$

In a many-body system with a total mass of M, the wavelength of the planetary-scale relativistic matter for a moving particle with the speed v becomes

$$\lambda = \frac{2\pi hM}{v}; \quad \psi = \exp(\frac{i}{hM}\int_0^x (u_1 dx_1 + u_2 dx_2 + u_3 dx_3 + u_4 dx_4)) \cdot \tag{8}$$

where h is a **Planck-constant-like constant**. Usually, the total mass M is approximately equal to the central-star's mass. It is found that this generalized matter wave works for quantizing orbits correctly for inner constituents in Fig.5. The key point is that the various systems have almost the same Planck-constant-like constant h in Table 1 with a mean value of 3.51e-16 $m^2s^{-1}kg^{-1}$, at least having the same order of magnitude!

5. Shells of Starlink Satellite altitudes

SpaceX's plans in 2019 were for the initial 12,000 satellites to orbit in three orbital shells: First shell: 1,440 in a 550 km (340 mi) altitude shell. Second shell: 2,825 Ku-band and Ka-band spectrum satellites at 1,110 km (690 mi). Third shell: 7,500 V-band satellites at 340 km (210 mi). In total, nearly 12,000 satellites were planned to be deployed, with (as of 2019) a possible later extension to 42,000 [34]. As shown in Fig.6.

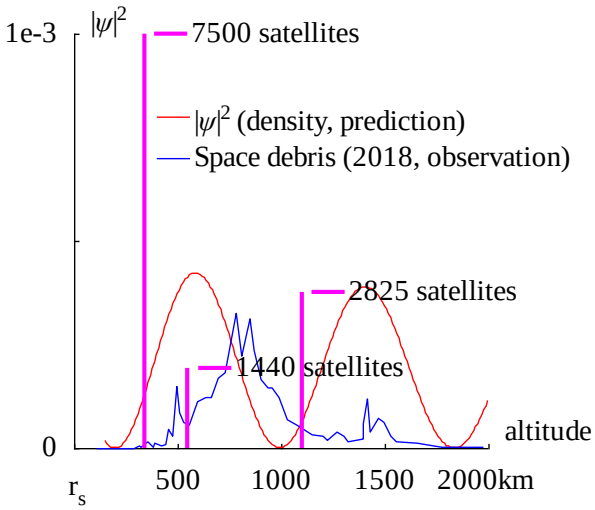

Fig.6 Satellite shell distribution of Starlink, 2019.

```
<Clet2020 Script>//Clet is a C compiler[26]
int i,j,k,m,n,N,nP[10]; double H,B,M,v_r,r,AU,r_unit,x,y,z,delta,D[10],S[10000];
double rs,rc,rot,a,b,atm_height,p,T,R1,R2,R3; char str[100];
int
Debris[96]={110,0,237,0,287,0,317,2,320,1,357,5,380,1,387,4,420,2,440,3,454,14,474,9,497,45,507,26,527,19,557,17,597,34,63
4,37,664,37,697,51,727,55,781,98,808,67,851,94,871,71,901,50,938,44,958,44,991,37,1028,21,1078,17,1148,10,1202,9,1225,6,
1268,12,1302,9,1325,5,1395,7,1395,18,1415,36,1429,12,1469,22,1499,19,1529,9,1559,5,1656,4,1779,1,1976,1,};
int Shell19[20]={550,0,550,1440, 1100,0,1110,2825,  340,0,340,7500,0};
int Shell20[40]={550,0,550,1440, 540,0,540,1440, 570,0,570,720, 560,0,560,336, 560,0,560,172,};
main(){k=80;rs=6.371e6;rc=0;atm_height=1.5e5;n=0; N=65;
H=1.956611e11;M=5.97237e24;AU=1.496E11;r_unit=1e4;
rot=2*PI/(24*60*60);//angular speed of the Earth
b=PI/(2*PI*rot*rs*rs/H); R1=rs/r_unit;R2=(rs+atm_height)/r_unit;R3=(rs+2e6)/r_unit;
for(i=R2;i<R3;i+=1) {r=abs(i)*r_unit; delta=2*PI*sqrt(GRAVITYC*M*r)/H;
y=SumJob("SLIT_ADD,@N,@delta",D); y=1e3*y/(N*N);// visualization scale:1000
if(y>1) y=1; S[n]=i;S[n+1]=y;n+=2;}
SetAxis(X_AXIS,R1,R1,R3,"altitude; r#sds#t;500;1000;1500;2000km ;");
SetAxis(Y_AXIS,0,0,1,"#if|ψ|#su2#t;0; ;1e-3;");DrawFrame(FRAME_SCALE,1,0xafffaf); x=R1+(R3-R1)/5;
SetPen(1,0xff0000);Polyline(n/2,S,x,0.8,"#if|ψ|#su2#t (density, prediction)");
for(i=0;i<48;i+=1) {S[i+i]=R1+(R3-R1)*Debris[i+i]/2000; S[i+i+1]=Debris[i+i+1]/300;}
SetPen(1,0x0000ff);Polyline(48,S,x,0.7,"Space debris (2018, observation) ");
SetPen(3,0xff4fff);Satellite();//Satellite2();
```

```
}
Satellite()
{for(i=0;i<3;i+=1) { j=i*4; D[0]=(Shell19[j]*1000+rs)/r_unit;D[1]=Shell19[j+1];
D[2]=D[0];D[3]=Shell19[j+3]/7500; Format(str,"%d satellites",Shell19[j+3]);
Polyline(2,D,D[0]+5,D[3],str);
}}
Satellite2()
{for(i=0;i<5;i+=1) { j=i*4; D[0]=(Shell20[j]*1000+rs)/r_unit;D[1]=Shell20[j+1];
D[2]=D[0];D[3]=Shell20[j+3]/7500; Format(str,"%d satellites",Shell20[j+3]);
Polyline(2,D,D[0]+5,D[3],str);
}}
#v07=?>A#t
```

Comparing to the distribution $|\psi|^2$ of the planetary-scale relativistic matter wave with the space debris distribution, the Starlink satellite shells run almost in the ranges of destructive interference of ψ, it means these orbits may need more energy and efforts to maintain their altitudes.

In April 2020, SpaceX modified the architecture of the Starlink network. SpaceX submitted an application to the FCC proposing to operate more satellites in lower orbits in the first phase than the FCC previously authorized. The first phase will still include 1,440 satellites in the first shell orbiting at 550 km (340 mi) in planes inclined 53.0 °, with no change to the first shell of the constellation launched largely in 2020:

First shell: 1,440 in a 550 km (341.8 mi) altitude shell at 53.0 °inclination

Second shell: 1,440 in a 540 km (335.5 mi) shell at 53.2 °inclination

Third shell: 720 in a 570 km (354.2 mi) shell at 70 °inclination

Fourth shell: 336 in a 560 km (348.0 mi) shell at 97.6 °inclination

Fifth shell: 172 satellites in a 560 km (348.0 mi) shell at 97.6 °inclination

SpaceX previously had regulatory approval from the FCC to operate another 2,825 satellites in higher orbits between 1,110 km (690 mi) and 1,325 km (823 mi), in orbital planes inclined at 53.8 °, 70.0 °, 74.0 °and 81.0 °[34].

Up to now, Starlink's effort of the modification and FCC seem in a direction that is not the expectation that this quantum gravity theory predicts. This quantum gravity theory suggests the Starlink constellation should be in constructive interference with the acceleration-roll wave [28].

6. Conclusions

In general, some quantum gravity proposals [1,2] are extremely hard to test in practice, as quantum gravitational effects are appreciable only at the Planck scale [3]. The early study [28-30] shown that ultimate acceleration can enhance the quantum gravity effects for test. In analogy with the ultimate speed c, there is an ultimate acceleration β, nobody's acceleration can exceed this limit β, in the solar system, β=2.956391e+10(m/s^2). Because this ultimate acceleration is a large number, any effect connecting to β will become easy to test, including quantum gravity tests. In this paper, an approach is put forward to connect the ultimate acceleration with quantum theory, as an application, the quantum gravity theory with the ultimate acceleration provides a useful formula to calculate the space debris distribution around the earth, in this paper the calculation results agree well with the experimental observation. Between February 2018 and 2022, SpaceX successfully launched 2,091 satellites into orbit. In March 2020, SpaceX reported producing six satellites per day. Comparing to the

space debris distribution, Starlink satellite altitudes are analyzed, some suggestions can be made to improve the Starlink constellation design and status by the quantum gravity theory with the ultimate acceleration.

References

[1]C. Marletto, and V. Vedral, Gravitationally Induced Entanglement between Two Massive Particles is Sufficient Evidence of Quantum Effects in Gravity, Phys. Rev. Lett., 119, 240402 (2017)
[2]T. Guerreiro, Quantum effects in gravity waves, Classical and Quantum Gravity, 37 (2020) 155001 (13pp).
[3]S. Carlip, D. Chiou, W. Ni, R. Woodard, Quantum Gravity: A Brief History of Ideas and Some Prospects, International Journal of Modern Physics D, V,24,14,2015,1530028. DOI:10.1142/S0218271815300281.
[4]de Broglie, L., CRAS,175(1922):811-813, translated in 2012 by H. C. Shen in Selected works of de Broglie.
[5]de Broglie, Waves and quanta, Nature, 112, 2815(1923): 540.
[6]de Broglie, Recherches sur la théorie des Quanta, translated in 2004 by A. F. Kracklauer as De Broglie, Louis, On the Theory of Quanta. 1925.
[7]NASA, https://solarscience.msfc.nasa.gov/interior.shtml.
[8]NASA, https://nssdc.gsfc.nasa.gov/planetary/factsheet/marsfact.html.
[9]B. Ryden Introduction to Cosmology, Cambridge University Press, 2019, 2nd edition.
[10]D. Valencia, D. D. Sasselov,R. J. O'Connell, Radius and structure models of the first super-earth planet, The Astrophysical Journal, 656:545-551, 2007, February 10.
[11]D. Valencia, D. D. Sasselov,R. J. O'Connell, Detailed models of super-earths: how well can we infer bulk properties? The Astrophysical Journal, 665:1413–1420, 2007 August 20.
[12]T. Guillot, A. P. Showman, Evolution of "51Pegasusb-like" planets, Astronomy & Astrophysics,2002, 385,156-165, DOI: 10.1051/0004-6361:20011624
[13]T. Guillot, A. P. Showman, Atmospheric circulation and tides of "51Pegasusb-like" planets, Astronomy & Astrophysics,2002, 385,166-180, DOI: 10.1051/0004-6361:20020101
[14]L.N. Fletcher,Y.Kaspi,T. Guillot, A.P. Showman, How Well Do We Understand the Belt/Zone Circulation of Giant Planet Atmospheres? Space Sci Rev, 2020,216:30. https://doi.org/10.1007/s11214-019-0631-9
[15]Y. Kaspi, E. Galanti, A.P. Showman, D. J. Stevenson, T. Guillot, L. Iess, S.J. Bolton, Comparison of the Deep Atmospheric Dynamics of Jupiter and Saturn in Light of the Juno and Cassini Gravity Measurements,Space Sci Rev, 2020, 216:84. https://doi.org/10.1007/s11214-020-00705-7
[16]Orbital Debris Program Office, HISTORY OF ON-ORBIT SATELLITE FRAGMENTATIONS, National Aeronautics and Space Administration, 2018, 15 th Edition.
[17]M. Mulrooney, The NASA Liquid Mirror Telescope, Orbital Debris Quarterly News, 2007, April,v11i2,
[18]Orbital Debris Program Office, Chinese Anti-satellite Test Creates Most Severe Orbital Debris Cloud in History, Orbital Debris Quarterly News, 2007, April,v11i2,
[19]A. MANIS, M. MATNEY, A.VAVRIN, D. GATES, J. SEAGO, P. ANZ-MEADOR, Comparison of the NASA ORDEM 3.1 and ESA MASTER-8 Models, Orbital Debris Quarterly News, 2021, Sept,v25i3.
[20]D. Wright, Space debris, Physics today,2007,10,35-40.
[21]TANG Zhi-mei, DING Zong-hua, DAI Lian-dong, WU Jian, XU Zheng-wen, "The Statistics Analysis of Space Debris in Beam Parking Model in 78 °North Latitude Regions," Space Debris Research, 2017, 17,3, 1-7.
[22]TANG Zhimei DlNG, Zonghua, YANG Song, DAI Liandong, XU Zhengwen, WU Jian The statistics analysis 0f space debris in beam parking model based On the Arctic 500 MHz incoherent scattering radar, CHINESE JOURNAL 0F RADIO SCIENCE, 2018, 25,5, 537-542
[23]TANG Zhimei , DING, Zonghua , DAI Liandong , WU Jian , XU Zhengwen, Comparative analysis of space debris gaze detection based on the two incoherent scattering radars located at 69N and 78N, Chin . J . Space Sci, 2018 38,1, 73-78. DOI:10.11728/cjss2018.01.073
[24]DING Zong-hua, YANG Song, JIANG hai, DAI Lian-dong, TANG Zhi-mei, XU Zheng-wen, WU Jian, The Data Analysis of the Space Debris Observation by the Qujing Incoherent Scatter Radar, Space Debris Research, 2018, 18,1, 12-19.
[25]YANG Song, DING Zonghua, Xu Zhengwe, WU Jian, Statistical analysis on the space posture, distribution, and scattering characteristic of debris by incoherent scattering radar in Qujing, Chinese Journal of Radio science, 2018 33,6 648-654, DOI:10.13443/j.cjors.2017112301
[26]Clet Lab, Clet: a C compiler, download at https://drive.google.com/file/d/1OjKqANcgZ-9V5 6rgcoMtOu9w4rP49sgN/view?usp=sharing
[27]Huaiyang Cui, Relativistic Matter Wave and Its Explanation to Superconductivity: Based on the Equality Principle, Modern Physics, 10,3(2020)35-52. https://doi.org/10.12677/MP.2020.103005
[28]Huaiyang Cui, Relativistic Matter Wave and Quantum Computer, Amazon Kindle ebook, 2021.
[29]Huaiyang Cui, (2023) Determination of Solar Radius and Earth's Radius by Relativistic Matter Wave, Journal of Applied Mathematics and Physics, 11:1, DOI: 10.4236/jamp.2023.111006
[30]Huaiyang Cui, (2023) Biological Clock of Relativistic Matter Wave and Calculation of Human Mean Lifespan 84 Years, Modern Physics (in Chinese), 2023, 13(2): 28-41. DOI: 10.12677/mp.2023.132005; Huaiyang Cui, (2023) Modelling of Human Lifespan -- Based on Quantum Gravity Theory with Ultimate Acceleration, viXra:2302.0121. https://vixra.org/abs/2302.0121
[31]N.Cox, Allen's Astrophysical Quantities, Springer-Verlag, 2001, 4th ed..
[32] S. E. Schneider, T. T. Arny, Pathways to Astronomy, McGraw-Hill Education, 2018, 5th ed.
[33] https://en.wikipedia.org/wiki/El_Ni%C3%B1o%E2%80%93Southern_Oscillation
[34] https://en.wikipedia.org/wiki/Starlink